

Antenna Doping: The Key for Achieving Efficient Optical Wavelength Conversion in Crystalline Chromophoric Heterolayers

Ritesh Haldar,* Hongye Chen, Antoine Mazel, Dong-Hui Chen, Gaurav Gupta, Navneet Dua, Stéphane Diring,* Fabrice Odobel,* and Christof Wöll*

High-yield wavelength conversion is one of the key requirements for efficient photon energy harvesting. Attempts to realize efficient conversion by simply stacking layers of chromophores have failed so far, even when using highly crystalline assemblies and employing the recently discovered long-range (>100 nm) Förster resonance energy transfer (LR-FRET). Optical conversion efficiency is drastically improved using chromophoric metal–organic framework heterolayers fabricated layer-by-layer in connection with an “antenna doping” strategy. Systematic investigations reveal that the LR-FRET mechanism, reported previously in chromophoric aggregates, is highly anisotropic for neat materials but can be made more isotropic by employing doping strategies. Using optimized fabrication parameters and dopant concentrations, a three-layer, two-step cascade with an overall optical conversion efficiency of $\approx 75\%$ is realized.

1. Introduction

Photon absorption and the subsequent transport of the resulting excitations are key steps in the conversion of light

to other forms of energy.^[1] For efficient light absorption, a huge variety of dyes is available, both from nature^[2] as well as from organic synthesis, with many of them relying on extended π -conjugated structures.^[3,4] To avoid reemission, the energy stored in the form of electronic excitations must be transported to regions in space where it can be converted into another form of energy, either chemical or electrical. In mesoscale assemblies, this exciton transport^[5] is often inefficient, since abundant unwanted interchromophore interactions lead to nonradiative deactivation or fluorescence quenching. Some of the commonly encountered loss processes result from H-type aggregate formation, structural defects, unwanted electron transfer (charge separation), etc.^[6,7] In order to avoid such losses upon energy transfer, high-purity and structurally perfect structures are required. Furthermore, established device architectures require a directional transport of excitons, as isotropic processes will greatly reduce device performance.^[8]

The most efficient transfer mechanism for singlet excitons is Förster resonance energy transfer (FRET). This mechanism allows the straightforward realization of a wavelength converter together with directional energy transport by arranging suitable donor–acceptor (D-A) pairs into a chain, e.g., consisting of three different chromophores C1, C2, and C3 as illustrated in **Figure 1a**. If the emission of C1 and the absorption of C2, as well as the emission of C2 and the absorption of C3, show sufficient spectral overlap, efficient FRET will cause the trimer to function as a two-step cascade in which the directed energy conversion of photons is absorbed in C1 via C2 to C3 (**Figure 1a,b**).


On the molecular level, a variety of organic synthesis schemes for the fabrication of such cascades have been reported, with most of them based on sophisticated coupling chemistry using suitable building blocks.^[9] However, for integration into organic photovoltaic (OPV) devices, mesoscopic assemblies providing transport on a macroscopic scale are mandatory.^[10] While a number of approaches have been presented to fabricate such chromophoric aggregates, e.g., based on zeolites,^[11] solvated molecules, gels (randomly oriented), or dendritic systems,^[12–16] only a few of these strategies are compatible with contemporary OPV device architectures. Moreover, most of these previously

Dr. R. Haldar, H. Chen, D.-H. Chen, G. Gupta, N. Dua, Prof. C. Wöll
Karlsruhe Institute of Technology (KIT)
Institute of Functional Interfaces (IFG)
Hermann-von-Helmholtz Platz-1
76344 Eggenstein-Leopoldshafen, Germany
E-mail: ritesh.haldar@kit.edu; christof.woell@kit.edu

H. Chen
State Key Laboratory of Mechanics and Control of Mechanical Structures
Key Laboratory for Intelligent Nano Materials and Devices of the MOE
Institute of Nano Science
Nanjing University of Aeronautics and Astronautics
Nanjing 210016, China

Dr. A. Mazel, Dr. S. Diring, Prof. F. Odobel
CNRS

Université de Nantes
CEISAM UMR 6230, Nantes F-44000, France
E-mail: stephane.diring@univ-nantes.fr; fabrice.odobel@univ-nantes.fr

 The ORCID identification number(s) for the author(s) of this article can be found under <https://doi.org/10.1002/admi.202100262>.

© 2021 The Authors. Advanced Materials Interfaces published by Wiley-VCH GmbH. This is an open access article under the terms of the Creative Commons Attribution-NonCommercial License, which permits use, distribution and reproduction in any medium, provided the original work is properly cited and is not used for commercial purposes.

DOI: 10.1002/admi.202100262

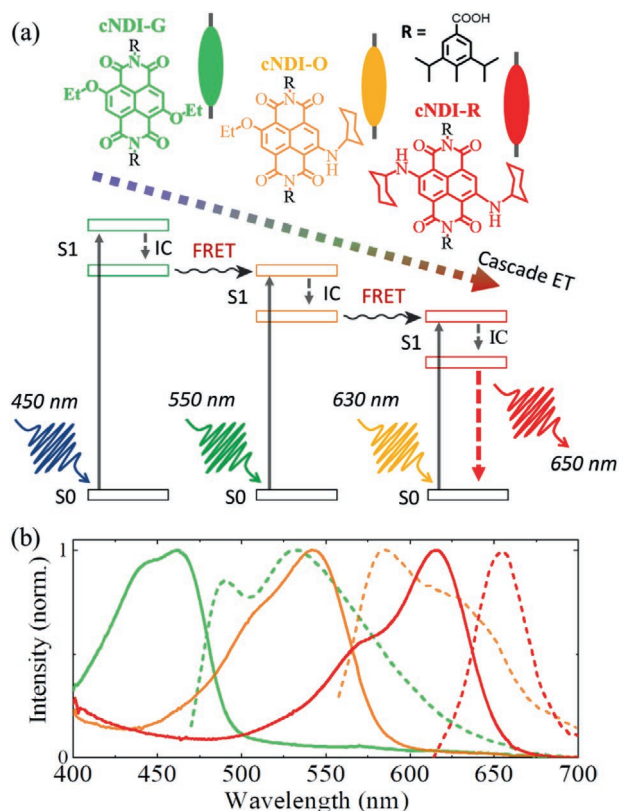


Figure 1. a) Schematic of a cascade FRET among cNDI-G, -O, and -R chemical structures of the linkers; the R group attached to the imide-N is a 3,5-diisopropylbenzoic acid (see the Supporting Information). b) Absorbance (solid) and fluorescence (dotted) spectra of Zn-cNDI-G, -O, and -R SURMOFs. All of the spectra are recorded at room temperature.

reported aggregates are limited by a fairly large number of structural imperfections, leading to quenching of excitons.

An emerging strategy for yielding chromophoric aggregates is based on metal–organic frameworks (MOFs), a large class of crystalline network materials originally introduced for applications in gas storage and separation.^[17–20] These porous coordination polymers have more recently been applied to optoelectronics, including light harvesting, photo-conductivity, nonlinear optics, etc.^[21–29] In particular, MOF thin films, SURMOFs, built from chromophoric linkers using layer-by-layer (lbl) methods, have been shown to allow for the construction of photoactive aggregates with well-defined photophysical properties and low defect densities. Such high optical quality MOF thin films were successfully used for photon upconversion,^[30] highly anisotropic directional transport of excitons,^[31] J-aggregate formation,^[32] and as an active medium in optical cavities.^[33,34]

Considering the requirements listed above for fabricating energy conversion cascades, it seems straightforward to follow the scheme depicted in Figure 1a to realize trilayer systems of chromophoric SURMOFs, since lbl methods are well suited to the fabrication of a hetero-multilayer.^[35] A particular advantage of chromophoric SURMOFs is the crystallinity and high degree of orientation of these thin films, resulting in very high absorption efficiency^[36] and the emergence of long-range anisotropic FRET transfer.^[37,38]

2. Results and Discussion

The approach presented here is based on three complementary core-substituted naphthalenediimide-based linkers (cNDIs; syntheses schemes are provided in the Supporting Information):^[39] bis-ethoxy-naphthalenediimide (cNDI-G), ethoxy-cyclohexylamine-naphthalenediimide (cNDI-O), and bis-cyclohexylamine-naphthalenediimide (cNDI-R) (Figure 1a). The absorption and emission profiles of these three dyes in the SURMOF structure show the spectral overlap of emission and absorption bands required for the realization of a two-step energy converter (Figure 1b and Figure S1, Supporting Information). The individual steps compose a FRET process: first, the blue-light-absorbing bottom cNDI-G layer, then a center cNDI-O, and finally a top layer of cNDI-R where the energy is emitted as red light. The individual chromophoric linkers were chosen such that, within a single MOF layer, they form J-aggregates (as reported previously, also the emission and absorption spectra are shown in Figure S2, Supporting Information and Figure 1b),^[6,32] an arrangement that is highly beneficial for yielding strong absorption and high-fluorescence quantum yields. The stacked trilayer SURMOF system was deposited on hydroxyl-terminated surfaces using an lbl spin-coating fabrication method, as described previously.^[32,40]

The basic MOF type used for the present study is Zn-SURMOF-2.^[41] The key structural elements of these reticular materials are ditopic dicarboxylate linkers, which are connected to Zn²⁺ ions yielding so-called paddle-wheels. These secondary building units then form 2D square-grid-like structures exhibiting a *P4* symmetry (Figure 2a). Using the liquid-phase epitaxy method with optimized parameters in connection with hydroxyl-terminated surfaces, we fabricated structurally well-defined Zn-SURMOF-2 thin films with [001] orientation, as shown in Figure 2a. The structure was the same for all three different chromophoric linkers (see the Experimental Section in the Supporting Information). The X-ray diffraction (XRD) data revealed that the three SURMOFs were isostructural (Figure 2b), with the cNDI-based linkers stacked along the [010] crystallographic direction (oriented parallel to the substrate) and an inter-linker distance of 6.8 Å.^[32] We thus conclude that the modification of the core substitution group in the NDI-linkers did not alter the unit cell parameters of these chromophoric crystalline structures,^[40] a key requirement for achieving good heteroepitaxial growth.

The 2D packing of the c-NDI chromophores results in the formation of J-aggregates^[32] with excellent lateral (intralayer) coupling. As a result of this pronounced structural anisotropy, Förster energy transport is very efficient parallel to the substrate^[31] but very poor (lower by a factor of 1000) perpendicular to the layers. The energy transfer perpendicular to the substrate is thus severely limited. This fact, which is a main obstacle for the realization of a conversion cascade, is demonstrated by the data shown in Figure S3a,b in the Supporting Information. Excitation of a bilayer heterostructure of Zn-cNDI-G/Zn-cNDI-O (HL-1) at 450 nm resulted in two emission bands, one at 530 nm from the bottom layer and one at 580 nm from the top layer. The presence of the 530 nm emission band from Zn-cNDI-G reveals that the energy transfer is inefficient—clearly a substantial fraction of the absorbed energy is not transferred to the top layer but reemitted from the bottom

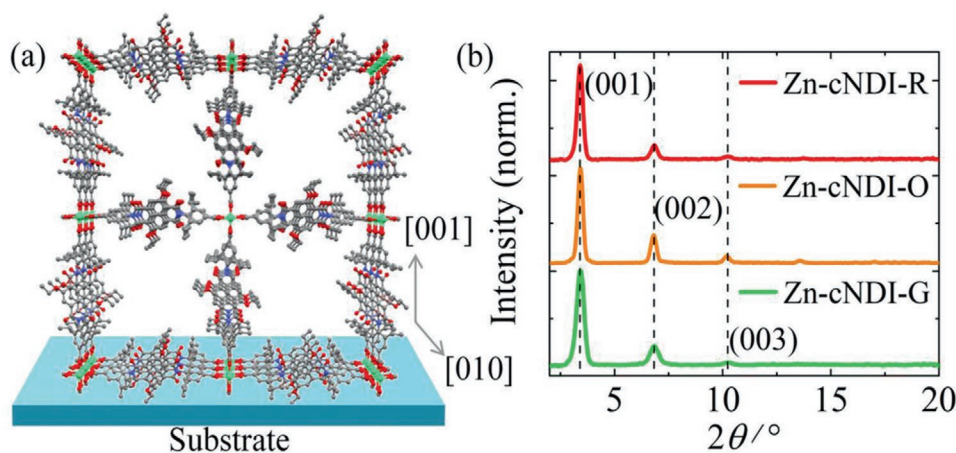


Figure 2. a) Zn-cNDI-G structure epitaxially grown along the (001) direction; b) out-of-plane XRD patterns of three Zn-SURMOF-2 films (green for Zn-cNDI-G, orange for Zn-cNDI-O, and red for Zn-cNDI-R).

SURMOF. In fact, the small amount of emission at 580 nm is not due to a small amount of energy transfer across the interface but to direct absorption of the 450 nm excitation light. This was demonstrated by the following experiment. We fabricated a test structure with an additional separator layer (≈ 80 nm FRET inactive layer) between Zn-cNDI-G and Zn-cNDI-O (see Figure S3a and HL-1-sep, Figure S4, Supporting Information). Since the separator should efficiently prohibit any FRET energy transfer, the observed emission at ≈ 580 nm unequivocally demonstrates that this emission results from direct excitation (Figure S3b, Supporting Information) and not from FRET transfer.

This observation makes clear that the main obstacle to realizing the conversion cascade is poor interlayer energy transfer. Although long-range FRET has been reported in such aggregated chromophoric systems in previous work,^[37,38] our results suggest that this transfer must be only within the layers, along the stacking directions. Obviously, the excellent crystalline order makes the energy transfer so anisotropic that interlayer coupling leading to energy transfer perpendicular to the substrate becomes impossible.

At this point, we speculated that the intentional introduction of defects allowing for a more isotropic coupling might be beneficial. Of course, such doping must avoid creating structural defects that could lead to unwanted quenching effects.^[42] Therefore, we introduced dopants in the form of different MOF linkers with the same length. The resulting structure, with “antennas” installed into the SURMOFs, is shown in Figure 3a. The bottom Zn-cNDI-G layer was doped with acceptor cNDI-O linkers, and the top Zn-cNDI-O layer with cNDI-R. Indeed, Figure 3b shows that this strategy was successful; the HL-2 SURMOF exhibited only a red emission at 630 nm upon excitation at 450 nm. The absence of any emission at 530 and 580 nm revealed that all the energy absorbed in the bottom layer was efficiently transferred to the upper cNDI-R layer; thus, a two-step conversion cascade was successfully realized.

The optimization of the antenna doping levels (i.e., the concentration of the emitter chromophores within the individual J-aggregate SURMOFs) to achieve maximum intralayer energy transfer was carried out as follows. First, the energy acceptor (emitter) cNDI concentration in the donor layer was enhanced

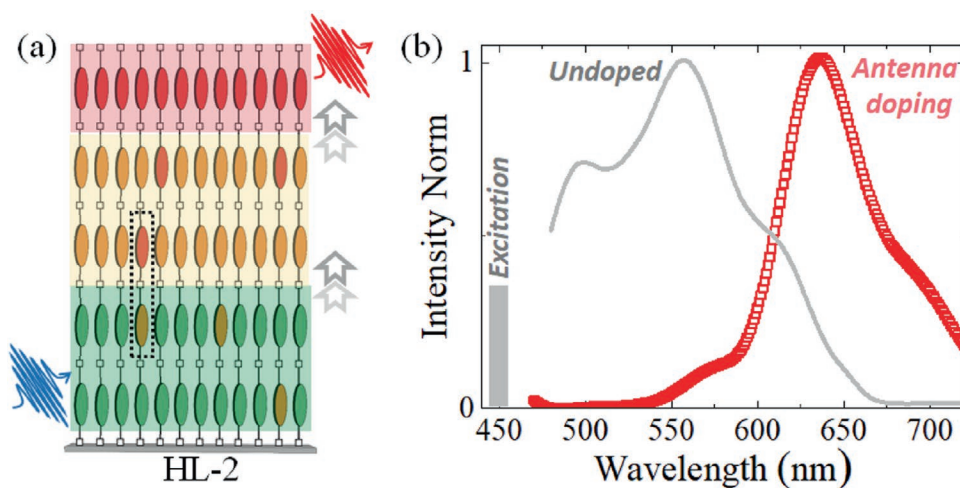


Figure 3. a) Schematic of the HL-2 heterostructure with antenna doping design. b) Emission spectrum of the HL-2 and a nondoped trilayer structure (HL-3), recorded upon excitation at 450 nm at room temperature.

until the donor emission was almost quenched, i.e., there was maximum energy transfer to the next layer. Figures S5 and S6 in the Supporting Information show the concentration-dependent emission spectra of those mixed-cNDI SURMOFs (Figure S7, Supporting Information). The energy transfer efficiency (as estimated from a comparison of the donor and acceptor emission intensities) amounted to 90% and 85% for the cNDI-O-doped Zn-cNDI-G and cNDI-R-doped Zn-cNDI-O layers, respectively. The high efficiency within the layer is expected because of strong intra-cNDI J-coupling. Based on these experiments, we chose 1.6% cNDI-O/Zn-cNDI-G as the bottom layer (thickness ≈ 20 nm), 1.9% cNDI-R/Zn-cNDI-O as the middle layer (thickness ≈ 20 nm), and Zn-cNDI-R as the top layer to construct a trilayer film HL-2 (Figure 3 and Figure S8a, Supporting Information). The excitation of HL-2 at 450 nm exhibited the absence of emission corresponding to the bottom layer Zn-cNDI-G and an intense emission from Zn-cNDI-R, demonstrating a high efficiency^[43,44] ($\approx 75\%$, estimated by comparison of the emission intensities of the individual chromophores in the SURMOF) cross-layer energy transfer to the top acceptor layer (Figure 3b and Figure S8b, Supporting Information). In the absence of the antenna dopants, a trilayer HL-3 (i.e., Zn-cNDI-G/Zn-cNDI-O/Zn-cNDI-R, 20 nm each layer) showed no red emission, indicating the absence of intralayer FRET (Figure 3b, gray line).

The observed efficient energy transfer is also evidenced by the following experiments: i) the excitation spectrum monitored at 640 nm (i.e., top layer, cNDI-R emission) showed a maximum corresponding to Zn-cNDI-G and Zn-cNDI-O, which indicates that the bottom layer energy is being transported to the top acceptor layer (Figure S9, Supporting Information); ii) a strong fluorescence intensity is observed with the 450 nm excitation compared to that with the 580 nm excitation (Figure S10, Supporting Information); and iii) a strong reduction of fluorescence lifetime at 500 nm reconfirmed the energy transfer (Figure S11, Supporting Information). The fluorescence quantum yield of HL-2 was found to be $\approx 10.5 \pm 1\%$, which is higher than that for pristine Zn-cNDI-G ($\approx 2.3 \pm 0.5\%$)^[32] and Zn-cNDI-R ($\approx 2.9 \pm 0.4\%$).

We rationalize the findings reported above by proposing that the antennas invoke LR-FRET also perpendicular to the layers. To confirm this hypothesis and to determine the range of this transfer process, we constructed a second set of model heterostructures (c-HL), similar to that described above. In this case, instead of neat chromophoric SURMOFs, doped MOF thin layers were used (see Figure S12a, Supporting Information, passive layer marked in gray). Figure S12b in the Supporting Information demonstrates that the emission from the top layer at 650 nm is intense in the absence of a separator (red) but weak for large separations (20 nm, black) (Figure S12b, Supporting Information). As expected for LR-FRET,^[37,38,45,46] the energy transfer occurs over rather far distances of >10 nm, which are substantially longer than those in normal FRET processes (see Figure S11, Supporting Information, showing fluorescence life-time quenching for the c-HL sample).

3. Conclusions

In conclusion, we demonstrated a two-step cascade for optical wavelength conversion by assembling three different cNDI

chromophores into heterolayer monolithic MOF thin films. Blue light was efficiently harvested and converted to red by transfer of excitons across two SURMOF heterointerfaces. To achieve high-yield, cross-layer FRET, we developed an “antenna doping” strategy. Introducing isolated FRET emitters within the anisotropic J-aggregates allowed us to overcome the strong directionality of the previously observed LR-FRET mechanism and to achieve efficient interlayer energy transfer. By optimizing the doping concentrations in the heterolayers, we could achieve i) $\approx 75\%$ energy conversion and ii) a fluorescence quantum yield enhancement of approximately four times compared to pristine individual SURMOFs. This new design strategy based on an Ibl heteroepitaxy process in combination with doping strategies opens up numerous options for optoelectronic device architectures.

Supporting Information

Supporting Information is available from the Wiley Online Library or from the author.

Acknowledgements

R.H. and H.C. contributed equally to this work. H.C. acknowledges financial support from China Scholarship Council (CSC, no. 201806830055); R.H. and C.W. acknowledge support from the Deutsche Forschungsgemeinschaft (DFG, German Research Foundation) under the Germany Excellence Strategy via the Excellence Cluster 3D Matter Made to Order (grant no. EXC-2082/1-390761711); and A.M., S.D., and F.O. acknowledge Région des Pays de la Loire through the program LUMOMAT for the financial support of this research with the project LumoMOF. S.D. is grateful for financial support from ANR PhotoMOF project, Grant ANR-18-CE05-0008-01. The authors greatly acknowledge J. Hémez and L. Arzel for mass spectrometry analysis at the AMaCC platform (CEISAM UMR CNRS 6230, University of Nantes).

Open access funding enabled and organized by Projekt DEAL.

Conflict of Interest

The authors declare no conflict of interest.

Data Availability Statement

Research data are not shared.

Keywords

crystalline chromophoric heterolayers, energy transfer, heterostructures, metal–organic frameworks

Received: February 19, 2021

Published online:

- [1] D. I. G. Bennett, K. Amarnath, G. R. Fleming, *J. Am. Chem. Soc.* **2013**, *135*, 9164.
- [2] G. D. Scholes, G. R. Fleming, A. Olaya-Castro, R. Van Grondelle, *Nat. Chem.* **2011**, *3*, 763.
- [3] A. Narita, X.-Y. Wang, X. Feng, K. Müllen, *Chem. Soc. Rev.* **2015**, *44*, 6616.

- [4] M. S. Vezie, S. Few, I. Meager, G. Pieridou, B. Döring, R. S. Ashraf, A. R. Goñi, H. Bronstein, I. McCulloch, S. C. Hayes, M. Campoy-Quiles, J. Nelson, *Nat. Mater.* **2016**, *15*, 746.
- [5] S. B. Penwell, L. D. S. Ginsberg, R. Noriega, N. S. Ginsberg, *Nat. Mater.* **2017**, *16*, 1136.
- [6] F. Würthner, T. E. Kaiser, C. R. Saha-Möller, *Angew. Chem., Int. Ed.* **2011**, *50*, 3376.
- [7] L. Cupellini, D. Calvani, D. Jacquemin, B. Mennucci, *Nat. Commun.* **2020**, *11*, 662.
- [8] M. Azzouzi, J. Yan, T. Kirchartz, K. Liu, J. Wang, H. Wu, J. Nelson, *Phys. Rev. X* **2018**, *8*, 031055.
- [9] K. Tsubaki, K. Takaishi, D. Sue, K. Matsuda, Y. Kanemitsu, T. Kawabata, *J. Org. Chem.* **2008**, *73*, 4279.
- [10] L. Lu, T. Zheng, Q. Wu, A. M. Schneider, D. Zhao, L. Yu, *Chem. Rev.* **2015**, *115*, 12666.
- [11] G. Calzaferri, S. Huber, H. Maas, C. Minkowski, *Angew. Chem., Int. Ed.* **2003**, *42*, 3732.
- [12] J. M. Serin, D. W. Brousmiche, J. M. Fréchet, *Chem. Commun.* **2002**, 2605.
- [13] V. Balzani, P. Ceroni, A. Juris, M. Venturi, S. Campagna, F. Puntoriero, S. Serroni, *Coord. Chem. Rev.* **2001**, 219, 545.
- [14] S. Diring, F. Puntoriero, F. Nastasi, S. Campagna, R. Ziessel, *J. Am. Chem. Soc.* **2009**, *131*, 6108.
- [15] K. V. Rao, K. K. R. Datta, M. Eswaramoorthy, S. J. George, *Chem. – Eur. J.* **2012**, *18*, 2184.
- [16] J. Liu, A. M. Kaczmarek, F. Artizzu, R. Van Deun, *ACS Photonics* **2019**, *6*, 659.
- [17] H. Furukawa, K. E. Cordova, M. O’Keeffe, O. M. Yaghi, *Science* **2013**, *341*, 1230444.
- [18] S. Kitagawa, R. Kitaura, S. I. Noro, *Angew. Chem., Int. Ed.* **2004**, *43*, 2334.
- [19] M. P. Suh, H. J. Park, T. K. Prasad, D.-W. Lim, *Chem. Rev.* **2012**, *112*, 782.
- [20] J.-R. Li, J. Sculley, H.-C. Zhou, *Chem. Rev.* **2012**, *112*, 869.
- [21] Z. Hu, B. J. Deibert, J. Li, *Chem. Soc. Rev.* **2014**, *43*, 5815.
- [22] D. M. D’Alessandro, *Chem. Commun.* **2016**, 52, 8957.
- [23] V. Stavila, A. Talin, M. Allendorf, *Chem. Soc. Rev.* **2014**, *43*, 5994.
- [24] J. Liu, W. Zhou, J. Liu, I. Howard, G. Kilibarda, S. Schlabach, D. Coupry, M. Addicoat, S. Yoneda, Y. Tsutsui, T. Sakurai, S. Seki, Z. Wang, P. Lindemann, E. Redel, T. Heine, C. Wöll, *Angew. Chem., Int. Ed.* **2015**, *54*, 7441.
- [25] T. Zhang, W. Lin, *Chem. Soc. Rev.* **2014**, *43*, 5982.
- [26] C. Y. Lee, O. K. Farha, B. J. Hong, A. A. Sarjeant, S. T. Nguyen, J. T. Hupp, *J. Am. Chem. Soc.* **2011**, *133*, 15858.
- [27] X. Liu, M. Kozłowska, T. Okkali, D. Wagner, T. Higashino, G. Brenner-Weiß, S. M. Marschner, Z. Fu, Q. Zhang, H. Imahori, S. Bräse, W. Wenzel, C. Wöll, L. Heinke, *Angew. Chem., Int. Ed.* **2019**, *58*, 9590.
- [28] R. Medishetty, J. K. Zareba, D. Mayer, M. Samoć, R. A. Fischer, *Chem. Soc. Rev.* **2017**, *46*, 4976.
- [29] I. Stassen, N. Burtch, A. Talin, P. Falcaro, M. Allendorf, R. Ameloot, *Chem. Soc. Rev.* **2017**, *46*, 3185.
- [30] M. Oldenburg, A. Turshatov, D. Busko, S. Wollgarten, M. Adams, N. Baroni, A. Welle, E. Redel, C. Wöll, B. S. Richards, I. A. Howard, *Adv. Mater.* **2016**, *28*, 8477.
- [31] R. Haldar, M. Jakoby, A. Mazel, Q. Zhang, A. Welle, T. Mohamed, P. Krolla, W. Wenzel, S. Diring, F. Odobel, B. S. Richards, I. A. Howard, C. Wöll, *Nat. Commun.* **2018**, *9*, 4332.
- [32] R. Haldar, A. Mazel, M. Krstić, Q. Zhang, M. Jakoby, I. A. Howard, B. S. Richards, N. Jung, D. Jacquemin, S. Diring, *Nat. Commun.* **2019**, *10*, 2048.
- [33] R. Haldar, L. Heinke, C. Wöll, *Adv. Mater.* **2020**, *32*, 1905227.
- [34] R. Haldar, Z. Fu, R. Joseph, D. Herrero, L. Martín-Gomis, B. S. Richards, I. A. Howard, A. Sastre-Santos, C. Wöll, *Chem. Sci.* **2020**, *11*, 7972.
- [35] R. Haldar, C. Wöll, *Nano Res.* **2020**, *14*, 355.
- [36] J. Jia, L. Gutiérrez-Arzaluz, O. Shekhah, N. Alsadun, J. Czaban-Jóźwiak, S. Zhou, O. M. Bakr, O. F. Mohammed, M. Eddaoudi, *J. Am. Chem. Soc.* **2020**, *142*, 8580.
- [37] Q. Zhang, C. Zhang, L. Cao, Z. Wang, B. An, Z. Lin, R. Huang, Z. Zhang, C. Wang, W. Lin, *J. Am. Chem. Soc.* **2016**, *138*, 5308.
- [38] S. M. Shaikh, A. Chakraborty, J. Alatis, M. Cai, E. Danilov, A. J. Morris, *Faraday Discuss.* **2019**, 216, 174.
- [39] N. Sakai, J. Mareda, E. Vauthey, S. Matile, *Chem. Commun.* **2010**, *46*, 4225.
- [40] R. Haldar, A. Mazel, R. Joseph, M. Adams, I. A. Howard, B. S. Richards, M. Tsotsalas, E. Redel, S. Diring, F. Odobel, C. Wöll, *Chem. – Eur. J.* **2017**, *23*, 14316.
- [41] J. Liu, B. Lukose, O. Shekhah, H. K. Arslan, P. Weidler, H. Gliemann, S. Bräse, S. Grosjean, A. Godt, X. Feng, K. Müllen, I.-B. Magdau, T. Heine, C. Wöll, *Sci. Rep.* **2012**, *2*, 921.
- [42] W. Schrimpf, J. Jiang, Z. Ji, P. Hirschle, D. C. Lamb, O. M. Yaghi, S. Wuttke, *Nat. Commun.* **2018**, *9*, 1647.
- [43] M. C. So, S. Jin, H.-J. Son, G. P. Wiederrecht, O. K. Farha, J. T. Hupp, *J. Am. Chem. Soc.* **2013**, *135*, 15698.
- [44] H. J. Park, M. C. So, D. Gosztola, G. P. Wiederrecht, J. D. Emery, A. B. F. Martinson, S. Er, C. E. Wilmer, N. A. Vermeulen, A. Aspuru-Guzik, J. F. Stoddart, O. K. Farha, J. T. Hupp, *ACS Appl. Mater. Interfaces* **2016**, *8*, 24983.
- [45] T. D. M. Bell, S. Yap, C. H. Jani, S. V. Bhosale, J. Hofkens, F. C. De Schryver, S. J. Langford, K. P. Ghiggino, *Chem. – Asian J.* **2009**, *4*, 1542.
- [46] J. Liu, L. Guillemeny, B. Abécassis, L. Coolen, *Nano Lett.* **2020**, *20*, 3465.